Materials Research Proceedings 41 (2024) 334-344 https://doi.org/10.21741/9781644903131-38

Multiscale Analysis of 316L stainless steel microstructures for WAAM manufacturing tool prediction

KROMER Robin[1,a *] and ARVIEU Corinne[1]

[1] I2M, UMR CNRS 5295, Université de Bordeaux, Arts et Métiers, Bordeaux INP, INRAe USC1368, France

[a] robin.kromer@u-bordeaux.fr

Keywords: WAAM, Stainless Steel, Microstructure, SDAS

Abstract. This study proposes a new approach on a multiscale analysis of 316L stainless steel microstructures to enhance the predictability and homogeneity of microstructure for the Wire Arc Additive Manufacturing (WAAM) process. Despite the promise in the fabrication of large-scale metallic components, achieving consistent microstructure and mechanical properties remains a challenge with WAAM. This research investigates the solidification behaviors, grain morphology, and mechanical characteristics of 316L stainless steel, aiming to develop a predictive framework for WAAM process optimization. By employing a systematic approach to the fabrication and subsequent analysis of 316L stainless steel walls, the study reveals critical insights into thermal gradients, solidification rates, and their impacts on microstructural features. The findings are anticipated to inform improved fabrication strategies, leading to enhanced mechanical properties and reliability in WAAM-manufactured components based on mereotopology philosophical framework. A spatio-temporal of the different tracks could be defined based on trajectory analysis.

Introduction

Wire Arc Additive Manufacturing (WAAM) is emerging as a revolutionary technology in the field of fabrication, promising to transform the production of large metallic structures [1]. As an additive manufacturing (AM) process, WAAM builds parts layer by layer, using an electric arc as the heat source and wire as the feed material. This method is not a novelty. It represents a significant leap forward in manufacturing large-scale parts, offering high deposition rates and lower costs compared to traditional manufacturing methods [2]. Specifically, when it comes to fabricating components from stainless steels, known for their robust mechanical properties and exceptional corrosion resistance, WAAM is particularly effective [3]. However, the metallurgy of stainless steel significantly contributes to its mechanical properties, such as resilience, resistance, and tenacity [4].

At the heart of WAAM technology is the electric arc, typically using the CMT technology from Fronius firm, which melts the metal wire feedstock [5]. As the molten metal is deposited, it solidifies to form a successive layer of the desired 3D object [6]. This process is repeated, stacking layers upon layers until the part is complete. As the metal is deposited, it undergoes rapid melting and solidification cycles, leading to non-equilibrium microstructures that can affect the mechanical properties of the final product [7]. For stainless steel components, in particular, maintaining the balance between austenite and ferrite phases in the microstructure is crucial to ensure the desired combination of strength, ductility, and corrosion resistance [8]. To address these challenges, researchers and practitioners are focusing on understanding the underlying physical metallurgy mechanisms of the WAAM process [9]. This involves studying the effects of process parameters such as heat input, cooling rate, and material feed rate on the microstructure and mechanical properties of the manufactured parts. For instance, the cooling rate during deposition significantly influences the formation and morphology of microstructures, including austenite and ferrite [10]. By optimizing these parameters, it is possible to control the microstructure and, consequently, the

mechanical properties of WAAM parts [11]. Another area of focus is the development of specific WAAM techniques to enhance the quality of stainless-steel parts. Techniques such as in-situ rolling combined with WAAM have shown promise in reducing anisotropy in the microstructure, thereby improving the uniformity of mechanical properties throughout the part. In vitro heat treatments, on the other hand, can help in relieving residual stresses and refining the microstructure, leading to better performance of the final component. Despite the progress made, achieving high-quality WAAM stainless steel parts remains a challenge due to the complexity of controlling the microstructure. The WAAM process leads to considerable anisotropy in both microstructure and mechanical properties, as the deposited layers cool and solidify at different rates [13]. This anisotropy can manifest in the form of residual stresses and distortion, affecting the dimensional accuracy and structural integrity of the components. Therefore, further research is needed to develop strategies to minimize these effects and produce components with uniform properties [14]. One promising strategy is the use of advanced monitoring and control systems during the WAAM process. For instance, defects in WAAM stainless steel parts, such as porosity, lack of fusion, or inclusions, can significantly compromise the integrity and performance of the components. These defects are typically attributed to sub-optimal process parameters or material feedstock quality. Advanced monitoring and control during the WAAM process can help in detecting and mitigating these defects early in the manufacturing process. Techniques such as real-time temperature monitoring and adaptive control systems adjust parameters on-the-fly to maintain optimal conditions, reducing the likelihood of defects [15].

To address the gap in understanding the influence of thermal management on microstructural evolution in WAAM processes, this study introduces a novel analysis of 316L stainless steel microstructures. Unlike existing works, which predominantly focus on qualitative descriptions, our approach leverages advanced quantitative methods to elucidate the relationship between process parameters and the formation of highly oriented columnar grains. This multidimensional analysis extends beyond mere equipment validation, offering new insights into optimizing heat input, cooling rates, and material feed rates for improved WAAM outcomes. The objectives are:

- To conduct an analysis of the microstructures. The study will focus on understanding the formation of large, highly oriented columnar grains dominated by epitaxial growth at the interface due to remelting
- To seeks to optimize the WAAM process strategy. This includes adjusting heat input, cooling rates and material feed rates. The research will develop a model to evaluate microstructure based on dwell time and interface between beads,

A spatio-temporal perspective is employed to use the information at a microscopic level linked to thermal gradient and solidification rate at different beads and their interaction. The research aims to demonstrate how these factors influence the microstructure from the bottom to the top location of the deposits, leading to finer microstructure in the upper zones and the gradual transition of the solidification mode.

Material, process and method description

Material

316L is an austenitic stainless-steel alloy known for its superior corrosion resistance and excellent mechanical properties at both room and high temperatures. The alloy typically contains 16-18% chromium, 10-14% nickel, and 2-3% molybdenum, along with small amounts of silicon, manganese, and carbon. The lower carbon content reduces susceptibility to sensitization when heated in the carbide precipitation range, which is especially beneficial in applications where the material is subjected to welding. The solidification of 316L during the process is complex and crucial in microstructure and, consequently, the mechanical properties of the produced part. The rapid melting and solidification cycles inherent in the WAAM process led to non-equilibrium microstructures typically characterized by fine dendritic structures and segregation of alloying

elements. At the interface of beads, composition can be different than in the beads itself. As the molten 316L solidifies, it typically forms a microstructure (Figure 1). The primary dendrites are often austenitic, with secondary phases possibly precipitating between the dendrites depending on the solidification conditions and the chemical composition of the alloy. The Primary Dendritic Arm Space (PDAS) and the Secondary Dendritic Arm Space (SDAS) are measured to enable gradient and solidification rate evaluation. The cooling rate significantly affects the dendrite arm spacing, with higher cooling rates leading to finer dendritic structures.

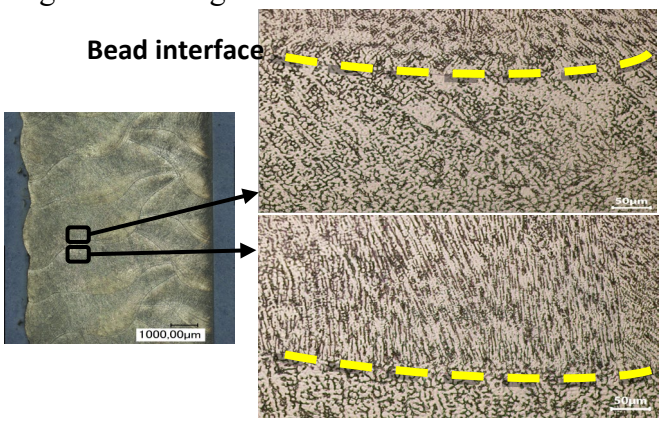

Figure 1: Beads interface with dendritic microstructure under the bead interface

WAAM

Process Parameters and Setup

The core of the WAAM setup is the arc welding system using CMT from Fronius (model 320i). The technology provides a low heat transfer and minimize the heat input, optimize arc stability, and provide good material deposition rate. A wire feeder is used to deliver the metal wire feedstock at a controlled rate into the arc, where it melts and gets deposited. The wire feed rate and the torch speed are set together to provide a specific weld track characterize by its width and height. To facilitate the layer-by-layer deposition, WAAM utilizes a gantry system that moves the welding torch along the predetermined path. The path speed is set to 15 mm/s. A 304L stainless steel support is used to support the workpiece (20mm thick plate Arc energy or heat input is a critical parameter as it influences the melt pool size, cooling rate, and consequently the microstructure of the deposit. It is determined by the voltage and current settings in the welding system. They are set to 227A and 17.5V. A balance needs to be struck between wire feed rate and path speed for sufficient deposition and build efficiency. The wire feed rate was set to 12 m/min. The shielding gas protects the molten metal from atmospheric contamination. For 316L, a mixture of argon with additions of carbon dioxide is commonly used (Ferroline gas- 92% Argon and 8% CO_2).

The samples are composed of three zones: one, three and four beads. The idea is to get different configurations between the interactions. It was one track. An interpass time of 60 seconds for each track (complete layer) was set. The first observed area is to get information for a single bead wall where there are no side effects. Then the second and third configurations are used to define the connectivity effects in heat transfer and microstructures. For the bead A, the cross-section 1,2 and 3 is then a unique and enable to compare the different interaction on the microstructure. It is true also for B, C and D respectively.

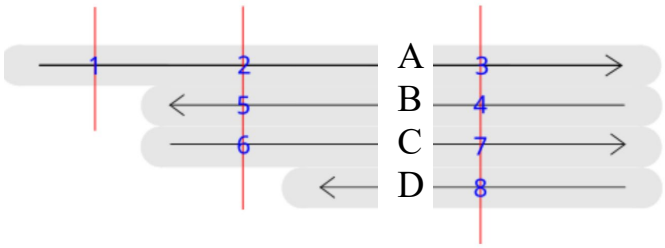

Figure 2: Configuration of the sample with tracks movement – red lines are the configuration for cross section observations

Sample Preparation:
Samples are typically extracted from various locations along the build direction across welding cross-sections of the path to capture the variance in microstructure between beads. The selected specimens are sectioned. Samples are meticulously prepared through mechanical polishing and chemical etching, a process essential for revealing microstructural features with high resolution for subsequent analysis. Chemical etching is performed to reveal the microstructural features (regal solution). An overview of the entire specimen cross-section is obtained by taking a series of micrographs, which are then stitched together to form a comprehensive image of the area (Figure 3). Python library is used to compute the interface length between different beads. The complete analysis is then calculated based on the total length that are localized together.

A/ 

B/ 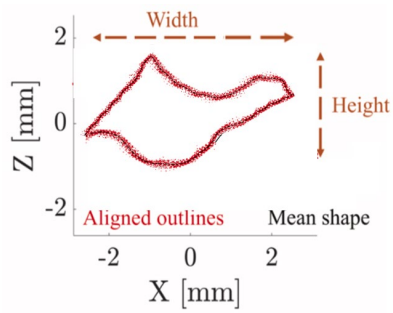

Figure 3: A/ Cross section 2 and B Coordinates of the interface of beads that are classified has the number 5

The microstructural analysis was conducted on a series of representative micrographs obtained from cross-sections of the alloy samples. SDAS were evaluated based on their visibility and structural integrity within the micrograph frame (Figure4). Measurements were limited to dendrite arms fully contained within the image to prevent partial measurement biases. The selection excluded any arms intersected by the image border. They are associated to the beads interface. A minimum of 12 secondary arms were analyzed per micrograph and per beads to ensure a statistically significant assessment of the SDAS, capturing the heterogeneity of the microstructural distribution. A grid of systematically oriented lines was digitally superimposed over the dendritic microstructure using image analysis tool in python. The center-to-center distance between consecutive secondary dendrite arms intersected by these lines was recorded. The variation of black and white enables to get the number and the check the consistency.

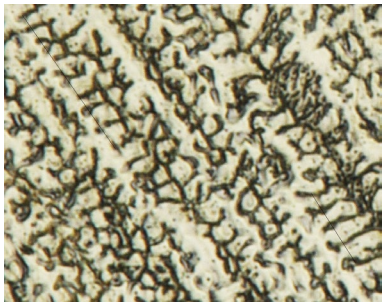

Figure 4: SDAS measurement based on micrography

Spatio-Temporal Analysis:

WAAM's heat dissipation modes transition from primarily conduction-based near the substrate to a blend of radiation and convection within the thin wall section as building progresses. This evolution significantly influences the cooling rate and solidification rate, impacting microstructure. Also, the overlapping of beads in WAAM is a common scenario, especially in multi-layer, multi-bead deposition. This overlapping significantly influences the local cooling rates and thermal gradients, leading to variations in microstructural features such as PDAS and SDAS. In the revised section titled 'Microstructural Evolution in WAAM,' we streamline our discussion to focus on the critical impact of dwell time and interface interaction between beads on grain orientation and size. This concise analysis underscores our contribution to refining WAAM process strategies through precise control over thermal gradients, directly influencing microstructural attributes and mechanical properties. On one hand, dwell time plays a critical role in this context, impacting the cooling rates and solidification rates, and thereby the microstructure. The transition from conduction-based to a blend of radiation and convection heat dissipation modes as building progresses not only influences cooling rates but also has a profound impact on the solidification rate and resulting microstructure. Dwell time directly impacts this transition. A longer dwell time allows for more heat to escape through conduction, potentially leading to a more uniform temperature distribution across the part. This uniformity can result in a more consistent microstructure. The cooling rate, which is directly influenced by the dwell time, plays a crucial role in determining the spacing of dendritic arms. A slower cooling rate, associated with shorter dwell times, tends to produce larger PDAS and SDAS, leading to a coarser microstructure. Conversely, longer dwell times can promote faster cooling rates, resulting in finer PDAS and SDAS and a more refined microstructure. The protocol enables to get on the different cross-sections and different configuration of dwell time as such there is two tracks (odd and even directions) (Figure 5).

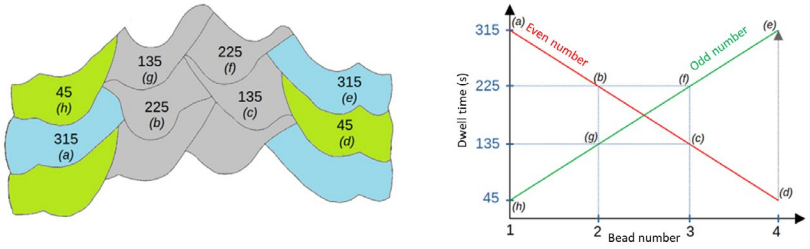

Figure 5: Dwell time for each configuration in the case of four beads (configuration 3)

On the other hand, in WAAM, each layer's cooling rate can be affected by its position in the sequence of deposition. Typically, even layers and odd layers exhibit different cooling behaviors due to the alternating deposition paths and the resulting variations in heat accumulation and dissipation. The differences in cooling rates between even and odd layers can lead to significant variations in microstructure across the build. To account for the differences in cooling rates between even and odd layers, a layer-specific cooling rate model can be developed and the interface of heat interaction need to be defined. This model would take into consideration the heat transfer mechanisms active in each layer, influenced by the layer's position and the history of heat input from previous layers. It means that the different interface length is computed based on micrography. Figure 6 present the interaction that have the bead 2. Interpass distance are define based on TOM method for continuous material deposition. So, the bead C remelt bead B (3→2 & 4→2), bead B remelt underneath bead B (5→2) and bead A remelt bead B (6→2). They are then classified based on the number of interactions. So, the heat from an adjacent bead can affect the thermal profile of its neighbors, leading to a more complex and less predictable cooling behavior. There is multi-dendrite structure direction near the interface due to multi-interaction. This interaction needs to be understood and modeled to predict its effect on microstructure.

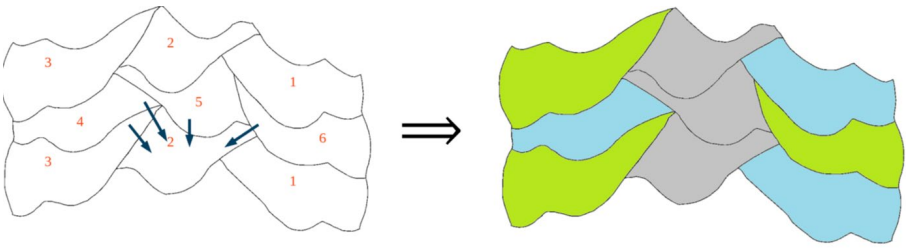

Figure 6: Heat flux for the for the bead 2 over time and classification of the beads based on heat flux number of interactions

Results

Microstructural analysis for one and third walls

The microstructural analysis focused on two specific sections: Section A1 (bead A and cross section 1) and the left line of Section A2 (bead A and cross section 2). These sections were chosen due to their differing thermal histories and positions within the WAAM build. A1 consists of a single bead wall, whereas A2 interacts with bead B. Figure 7 highlights the SDAS measured across these sections, providing a snapshot of the microstructural variations within the WAAM wall. The consistent SDAS measurements in Section A1 suggest a uniform cooling rate, highlighting the efficacy of maintaining stable process parameters (Figure 7.A). This uniformity can be attributed to consistent manufacturing parameters and the location of the section within the build, likely away from more complex geometric features or overlapping bead regions. For the left line of Section A2, SDAS measurements indicated a higher degree of variability. This variability could be due to the complex interplay of thermal histories in this section, influenced by overlapping beads and varying bead geometries. As this section is likely closer to the wall's edge or features more bead overlaps, the resultant thermal gradients would be more variable, leading to diverse cooling rates and, consequently, a more heterogeneous microstructure. An intriguing aspect of the study, as presented in Figure 7.B, was the examination of SDAS variability based on the parity of the layers in Section A1 and the left line of Section A2. This analysis aimed to understand how the alternating deposition strategy (even and odd layers) impacts the microstructure. On one hand, in even-numbered layers, the SDAS values tended to be more uniform, suggesting a more consistent cooling rate. This uniformity might be due to the repetitive nature of the deposition process, where even layers experience similar thermal histories. On the other hand, the odd-numbered layers exhibited more variation in SDAS values. This finding suggests that the cooling rates in these

layers are less consistent, possibly due to variations in bead overlap or changes in the thermal environment as the build progresses. The odd layers are possibly more influenced by the cumulative heat input and varying bead geometries. Regions with finer SDAS are expected to exhibit higher strength and potentially better fatigue resistance due to their refined microstructure. In contrast, areas with coarser SDAS might have lower strength but potentially better ductility. This microstructural analysis underscores the complexity of predicting and controlling the microstructure in WAAM processes. The variability in SDAS across different sections and layers reflects the intricate interplay of thermal dynamics during the build and material anisotropy.

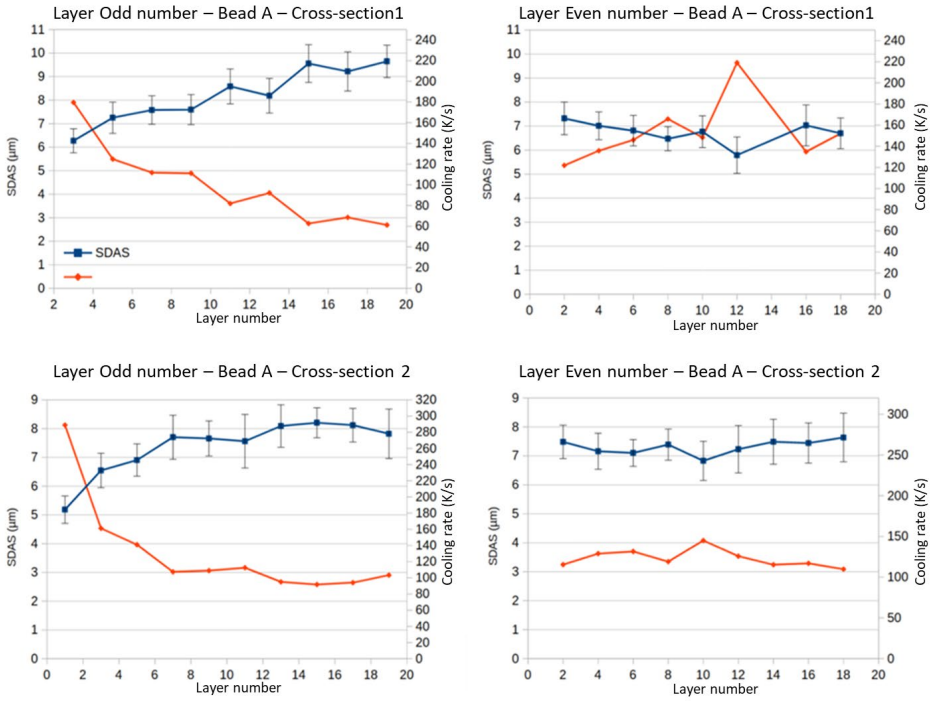

Figure 7: SDAS and Cooling rate at each layer for Bead A and cross section 1 and 2 for comparison (divided into odd and even layers)

Integration of Bead Interface, Dwell Time, and SDAS in WAAM

As new material is deposited, it interacts thermally with the previously deposited bead (remelting bead), affecting the overall heat dissipation dynamics. The surface area of this interface is directly proportional to the amount of the interaction and is a signature of the heat that was conducted away during the thermal ageing effects. In addition, dwell time, the waiting period between the deposition of successive layers or beads, allows for the reduction of residual heat in the part. Longer dwell times facilitate greater heat dissipation, leading to lower local temperatures at the time of subsequent bead deposition. This cooling effect influences the solidification rate of the new layer, directly impacting the formation of dendritic structures. Based on the dwell time analysis of each beads and section configurations, SDAS were measures following the micrography protocol. These quantified values of SDAS were then correlated with the dwell time and interface area to analyze their effects on microstructural characteristics. The number of beads was considered due to observed variations in SDAS from the bottom to the top. Odd and even number were also used. The regression meta model provides a Mean Predictive Average of 0.91(R^2) of prediction (Bayesian model with Pycaret library tool). The accompanying feature importance plot (Figure 8) elucidates the relative significance of various parameters in the predictive model for 3D printing process optimization. Dwell time emerges as the most influential factor, with a variable importance value of approximately 0.61, underscoring its pivotal role in

determining the microstructural characteristics of the printed material. This is in alignment with the thermal control hypothesis, where the dwell time governs the rate of heat dissipation, subsequently affecting the solidification dynamics and the evolution of the dendritic structures. The interface length, representing the contact area between successive layers, holds a variable importance of around 0.21. This parameter is indicative of the thermal interaction at the interface, which can influence the microstructure due to localized remelting and cooling cycles. The number of beads, though less significant with a variable importance close to 0.13, still contributes to the model's predictive capacity. This factor likely represents the cumulative effect of layering in the build process, influencing the overall thermal profile and gradient experienced by the material. Lastly, the variable labeled 'Order' exhibits minimal importance, suggesting that the sequence of deposition has a negligible direct impact on the microstructure as captured by the model.

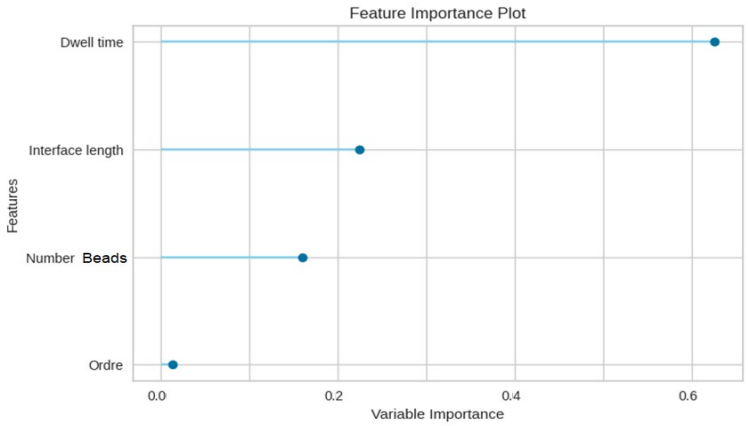

Figure 8: Feature importance (%) based on metamodel generation

Discussion

The influence of thermal gradients and solidification rates on grain morphology is crucial because they dictate the cooling speed and, consequently, the microstructural features. For instance, faster cooling rates typically result in finer grains, enhancing the material's mechanical properties. This aspect is pivotal as it directly affects the mechanical properties of the printed material. The central argument here is that by controlling these parameters, it's possible to achieve a more predictable and uniform microstructure. Presented by Wang et al. [5], the arc energy transfer is the key point of the microstructure and mechanical behaviors. Heat input is directly link to finer structure. Also, the interface lead to microstructure population variation such as it was presented by the model. Belotti et al. [14] presented that the solidification structure of the WAAM part contains γ-austenite and δ-ferrite, as empirically described by constitution diagrams. An EDX analysis needs to be perform to check also the impact on the composition based on different heat interaction configuration and confirm with a literature review.

Secondly, Guang et al [16] found that using shielding gases that result in higher heat input reduces the amount of retained austenite in the as-deposited microstructure. It has been demonstrated that the required tensile properties can be achieved by applying post-deposition heat treatment. However, it is suggested that direct aging in as deposited condition resulted of harmful intermetallic phases which embrittles the deposit. It means that a lot of environment effects can have influence on localize variation. Also heat treatments over the complete part is a key to eventually control microstructure homogeneity and it is shape dependent. It should be necessary to check their effects on the model prediction with a checking when it goes from four bead to three or two beads.

Finally, employing a mereotopological approach allows for a nuanced analysis of the material's behavior, tracing the continuous and discrete interactions within the WAAM process. This aids in developing predictive models that accurately simulate the effects of varying process parameters on the microstructure. The key argument here is that mereotopology aids in a deeper and more nuanced understanding of the material's trajectory and behavior, taking into consideration the interface interaction. The model can be used to predict the microstructure composition of different beads based on trajectory analysis. The mereotopological equation:

$$\begin{aligned} &WAAM\_system := \exists \{ MoltenPool, WireFeed, Arc, Substrate \} \\ &\quad \{ (MoltenPool\ X\ WireFeed \wedge MoltenPool\ O\ Substrate) \wedge \\ &\quad ((Temperature \oplus CoolingRate) \wedge (FeedSpeed \otimes ArcStability)) \wedge \\ &\quad F(FeedSpeed, CoolingRate)\} \end{aligned} \tag{1}$$

It integrates key components like the molten pool, wire feed, arc, and substrate, each playing a vital role in the deposition process. The equation's structure reflects the complex dynamics of Wire Arc Additive Manufacturing (WAAM), where the behavior of each component influences the final product's quality. The interaction between the molten pool and wire feed (MoltenPool X WireFeed) is crucial in determining bead formation, directly influenced by factors such as dwell time – the duration the arc focuses on a specific area. Dwell time affects the heat input, influencing the cooling rate and ultimately the microstructure of the material. The overlap between the molten pool and the substrate (MoltenPool O Previous layer) represents the interface interaction between successive beads, a critical factor in ensuring mechanical strength and integrity of the final product. The behavioral operators in the equation, such as (Temperature $\oplus$ CoolingRate) and (FeedSpeed $\otimes$ ArcStability), denote the allowable variations in temperature and cooling rates, and the necessity of maintaining consistent feed speed and arc stability, respectively. These factors are fundamental in controlling the trajectory of the deposition process, impacting the microstructural properties of the manufactured material. Furthermore, the predictive function F(FeedSpeed, CoolingRate) in the equation represents the feedback mechanisms that link process parameters such as feed speed and cooling rates to the system's behavior over time. The development of predictive models, as evidenced by our findings, marks a significant step towards process control in WAAM. For example, by incorporating dwell time and interface measurements into our models, we can predict with high accuracy the resulting microstructure. Such predictive capability allows for real-time adjustments to process parameters, potentially saving significant resources and time.

Conclusion

Our study culminates in a conclusion that succinctly encapsulates the significant advancements made in the predictive modeling of WAAM processes. By articulating the practical implications of our findings, we underscore the potential for these models to revolutionize the manufacturing of 316L stainless steel components, offering a pathway towards optimized, cost-effective production methods. The study led to the development of predictive models that utilize interface measurements, dwell time evaluation, and bead classification to optimize WAAM processes. It enables an advancement in optimizing WAAM processes. The interface and dwell time are associated with SDAS, which can then contribute to a more accurate and controlled method of manufacturing. This research highlights the importance of detailed microstructural analysis and its correlation with process parameters. Dwell time is a key point to enhance microstructure homogeneity. It is also important to optimize inter-path width to get homogeneous interface between beads. Heat accumulation also influence of the anisotropy. The development of predictive models based on the study's findings is a first step in process control advancement. The primary argument for these models is their potential to significantly reduce the trial and error typically associated with WAAM processes. By accurately predicting how changes in process parameters

affect the microstructure of materials, these models can permit control of the manufacturing process, enhance efficiency, and reduce costs. This mereotopological approach, therefore, stands as a groundbreaking method in the field of additive manufacturing, offering a comprehensive way to understand and manipulate the complex interplay of various factors that determine the quality and properties of the final product.

References

[1] Korkmaz, M.E., Waqar, S., Garcia-Collado, A., Gupta, M.K., Krolczyk, G.M. (2022). A technical overview of metallic parts in hybrid additive manufacturing industry. Journal of Materials Research and Technology, 18, 384-395. https://doi.org/10.1016/j.jmrt.2022.08.074

[2] Huang, S.H., Liu, P., Mokasdar, A., Hou, L. (2013). Additive manufacturing and its societal impact: a literature review. International Journal of Advanced Manufacturing Technology, 67(5), 1191-1203.

[3] Queguineur, A., Rückert, G., Cortial, F., Hascoët, J. (2018). Evaluation of wire arc additive manufacturing for large-sized components in naval applications. Welding World, 62(2), 259-266. https://doi.org/10.1007/s40194-017-0533-7

[4] Vora, J., Parmar, H., Chaudhari, R., Khanna, S., Doshi, M., Patel, V. (2022). Experimental investigations on mechanical properties of multi-layered structure fabricated by GMAW-based WAAM of SS316L. Journal of Materials Research and Technology,20, 2748-2757. https://doi.org/10.1016/j.jmrt.2022.08.074

[5] Wang, L., Xue, J., Wang, Q. (2019). Correlation between arc mode, microstructure, and mechanical properties during wire arc additive manufacturing of 316L stainless steel. Materials Science and Engineering: A, 751, 183-190. https://doi.org/10.1016/j.msea.2019.02.078

[6] Rosli, N.A., Alkahari, M.R., Abdollah, M.F.B., Maidin, S., Ramli, F.R., Herawan, S.G. (2021). Review on effect of heat input for wire arc additive manufacturing process. Journal of Materials Research and Technology, 11, 2127-2145. https://doi.org/10.1016/j.jmrt.2021.04.067

[7] Yadollahi, A., Shamsaei, N., Thompson, S.M., Seely, D.W. (2015). Effects of process time interval and heat treatment on the mechanical and microstructural properties of direct laser deposited 316L stainless steel. Materials Science and Engineering: A, 644, 171-183. https://doi.org/10.1016/j.msea.2015.07.056

[8] PS, G., S, J., DT, S. (2023). Influence of heat input on microstructure and mechanical behaviour of austenitic stainless steel 316L processed in wire and arc additive manufacturing. Proceedings of the Institution of Mechanical Engineers, Part E: Journal of Process Mechanical Engineering, 237(2), 149-161. https://doi.org/10.1177/09544089221100214

[9] Aldalur, E., Suarez, A., Veiga, F. (2022). Thermal expansion behaviour of Invar 36 alloy parts fabricated by wire-arc additive manufacturing. Journal of Materials Research and Technology, 19, 3634-3645.

[10] Chaudhari, R., Parmar, H., Vora, J., Patel, V.K. (2022). Parametric Study and Investigations of Bead Geometries of GMAW-Based Wire–Arc Additive Manufacturing of 316L Stainless Steels. Metals, 12, 1232.

[11] Wang, C., Liu, T.G., Zhu, P., Lu, Y.H., Shoji, T. (2020). Study on microstructure and tensile properties of 316L stainless steel fabricated by CMT wire and arc additive manufacturing. Materials Science and Engineering: A, 796. https://doi.org/10.1016/j.msea.2020.140006

[12] Elmer, J.W., Fisher, K., Gibbs, G., Sengthay, J., Urabe, D. (2022). Post-build thermomechanical processing of wire arc additively manufactured stainless steel for improved

mechanical properties and reduction of crystallographic texture. Additive Manufacturing, 50. https://doi.org/10.1016/j.addma.2021.102573

[13] Singh, S., Jinoop, A.N., Kumar, T.G.T., Palani, I.A., Paul, C.P., Prashanth, K.G. (2021). Effect of Interlayer Delay on the Microstructure and Mechanical Properties of Wire Arc Additive Manufactured Wall Structures. Materials (Basel), 14(15), 4187. https://doi.org/10.3390/ma14154187

[14] Belotti, L.P., van Dommelen, J.A.W., Geers, M.G.D., Ya, W., Hoefnagels, J.P.M. (2024). Influence of the printing strategy on the microstructure and mechanical properties of thick-walled wire arc additive manufactured stainless steels. Journal of Materials Processing Technology, 324.

[15] Baier, D., Wolf, F., Weckenmann, T. et al. Thermal process monitoring and control for a near-net-shape Wire and Arc Additive Manufacturing. Prod. Eng. Res. Devel. 16, 811–822 (2022).

[16] Guang Y., Fangbin D., Siyu Z., Bin W., Lanyun Q., Jianshen Z., Influence of shielding gas nitrogen content on the microstructure and mechanical properties of Cu-reinforced maraging steel fabricated by wire arc additive manufacturing,Materials Science and Engineering: A, 832,2022, https://doi.org/10.1016/j.msea.2021.142463